INDIRECT BOUNDARY ELEMENT METHOD FOR CALCULATION OF POTENTIAL FLOW AROUND A PROLATE SPHEROID

Ghulam Muhammad[1*], Nawazish Ali Shah[1] and Muhammad Mushtaq[1]

[1] Department of Mathematics, University of Engineering & Technology Lahore – 54890, Pakistan
Corresponding Author, e-mail: g_muhammad123@hotmail.com

Abstract:

In this paper, an indirect boundary element method (IDBEM) is applied to calculate an incompressible potential flow around a prolate spheroid using linear boundary elements and such potential flow around a prolate spheroid is calculated using different numbers of boundary elements to approximate the body surface.. In this case, the indirect boundary element method with dipoles distribution is used. IDBEM is based on the distribution of singularities, such as sources or dipoles over the boundary of the body and computes the unknowns in the form of singularity strengths. With indirect boundary element method one can choose a singularity type to best model a given system. IDBEM is popular due to its simplicity and it is more general and flexible for the solution of a given problem. A comparison study between computed results for velocity distribution and analytical results is made and it can be seen from tables and graphs that the computed results for velocity distribution are seen to be quite good in agreement with the analytical results for the problem under observation.

Keyword: indirect direct boundary element method, potential flow, axisymmetric flow, steady flow, prolate spheroid.

Introducton:

The boundary element method (BEM) is a numerical technique consisting of sub-diving the surface of the fluid flow field into a series of discrete elements over which the function can vary and it has been progressing for the last forty years due to its simplicity and efficiency. Such method is gaining popularity day by day among the computational and engineering communities. The term boundary element method opened eyes in the department of civil engineering, Southampton University, United Kingdom (Brebbia,C.A,1978). In literature, these methods existed under different names such as ‘panel methods’, ‘surface singularity methods’, ‘boundary integral equation methods’ or ‘boundary integral solutions’. In the past, finite difference method (FDM) and finite element method, etc. (Hirt,C.W.et al,1978, Markatos,N.G,1983, Demuran,A.O.et al,1982 and Ecer,A.,1982) were being used to find the numerical solutions of problems in computational fluid dynamics. But the boundary element methods offer important advantages over the domain type methods. One of the advantages is that with boundary element methods one has to define the whole surface of the body, whereas with domain methods it is necessary to discretize the entire flow field. So, it is easier to use, economical, cost effective and time saving due to small data than the other competing computational methods i.e. finite difference and finite element methods etc. The most important

characteristics of these methods are the much smaller system of equations and considerable reduction in data , which are perquisite to run a computer program efficiently. Furthermore, boundary element methods are well suited to flow problems with infinite domains. The boundary element methods can be classified into direct and indirect boundary element methods. The direct method takes the form of a statement, which provides the values of unknown variables at any flow field point in terms of the complete set of all the boundary data The equation of direct method can be formulated using either as an approach based on Green's function (Lamb,H,1932, Milne-Thomson,L.M,1968, Kellogg,O.D,1929) or a particular case of the weighted residual methods (Brebbia,C.A. and Walker,S,1980). BEMs are classified as 'indirect' and 'direct' methods. The indirect method utilizes a distribution of singularities over the boundary of the body and computes this distribution as the solution of integral equation and the equation indirect method can be derived from that of direct method. The flow fields around three-dimensional bodies were calculated by using a lower-order indirect method (Hess,J.L.and Smith,A.M.O,1962,1967). The direct method was applied for calculating the potential flow problems (Morino.L.et al,1975). Boundary element methods are essential the methods for solving partial differential equations (PDEs) arising in problems in such diverse topics as stress analysis, heat transfer and electromagnetic theory, potential theory, fracture mechanics, fluid mechanics, elasticity, elastostatics and elastodynamics, etc. (Muhammad,G,.et al,2009). These methods are also being used for the solution of incompressible flows around complex configurations. Thus the boundary element methods are powerful numerical techniques receiving much attention from computational researchers and engineering community, which are offering the numerical solutions of a large number of flow problems of different types and the computational cost, labor and time in these methods are much smaller than other computational methods.

Flow past a prolate spheroid:

Let a prolate spheroid be generated by rotating an ellipse with semi – major axis 'a' and semi – minor axis 'b' about its major axis and let a uniform stream of velocity U be in the positive direction of z – axis as shown in figure (1) (Shah,N.A.,2008) .

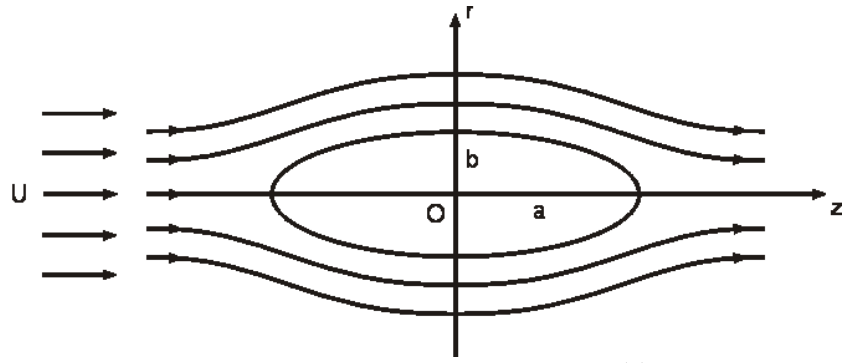

Figure (1)

The Prolate spheroid is defined by the transformation

$$z + i\,r = c\cosh\zeta = c\cosh(\xi + i\eta) = c\cosh\xi\cosh(i\eta) + c\sinh\xi\sinh(i\eta)$$

$$= c\cosh\xi\cos\eta + i\,c\sinh\xi\sin\eta$$

Comparison of real and imaginary parts gives

$$z = c \cosh \xi \cos \eta , \quad r = c \sinh \xi \sin \eta \tag{1}$$

Therefore the curve $\xi = \xi_0$ is an ellipse in the $z\,r$ – plane whose semi – axes are

$$\left.\begin{aligned} a &= c \cosh \xi_0 \\ b &= c \sinh \xi_0 \end{aligned}\right] \tag{2}$$

and so $\xi = \xi_0$ is a Prolate spheroid .

The stream function ψ for a Prolate spheroid moving in the negative direction of the z – axis with velocity U is given by

$$\psi = \frac{\frac{1}{2} U b^2 \left(\cosh \xi + \sinh^2 \xi \ln \tanh \frac{\xi}{2} \right) \sin^2 \eta}{\frac{a}{c} + \frac{b^2}{c^2} \ln \frac{a + b - c}{a + b + c}} \tag{3}$$

Also , the stream function ψ for the uniform stream with velocity U , in the positive direction of z – axis is given by

$$\psi = -\frac{1}{2} U r^2$$

Therefore the stream function ψ for the streaming motion past a fixed Prolate spheroid in the positive direction of the z – axis becomes

$$\psi = -\frac{1}{2} U r^2 + \frac{\frac{1}{2} U b^2 \left(\cosh \xi + \sinh^2 \xi \ln \tanh \frac{\xi}{2} \right) \sin^2 \eta}{\frac{a}{c} + \frac{b^2}{c^2} \ln \frac{a + b - c}{a + b + c}} \tag{4}$$

which on using (1) becomes

$$\psi = -\frac{1}{2} U c^2 \sinh^2 \xi \sin^2 \eta + \frac{\frac{1}{2} U b^2 \left(\cosh \xi + \sinh^2 \xi \ln \tanh \frac{\xi}{2} \right) \sin^2 \eta}{\frac{a}{c} + \frac{b^2}{c^2} \ln \frac{a + b - c}{a + b + c}} \tag{5}$$

To determine the formula for the velocity , the following relation is used (Shah,N.A.,2008)

$$V^2 r^2 f'(\zeta) \bar{f}'(\bar{\zeta}) = \left(\frac{\partial \psi}{\partial \xi} \right)^2 + \left(\frac{\partial \psi}{\partial \eta} \right)^2 \tag{6}$$

Since $f(\zeta) = c \cosh(\zeta)$

$$f'(\zeta) = c \sinh(\zeta) = c \sinh(\xi + i\eta), \quad \bar{f}'(\bar{\zeta}) = c \sinh(\xi - i\eta)$$

and $$f'(\zeta) \bar{f}'(\bar{\zeta}) = c^2 (\sinh^2 \xi \cos^2 \eta + \cosh^2 \xi \sin^2 \eta) \tag{7}$$

When $\xi = \xi_0$, then from (1) , (6) and (7)

$$V^2 c^4 \sinh^2 \xi_0 \sin^2 \eta (\sinh^2 \xi_0 \cos^2 \eta + \cosh^2 \xi_0 \sin^2 \eta) = \left(\frac{\partial \psi}{\partial \xi} \right)^2_{\xi = \xi_0} + \left(\frac{\partial \psi}{\partial \eta} \right)^2_{\xi = \xi_0} \tag{8}$$

Now from (5) , we get

$$\left(\frac{\partial \psi}{\partial \xi}\right)_{\xi=\xi_0} = -U c^2 \sinh \xi_0 \cosh \xi_0 \sin^2 \eta + \frac{U b^2 \left(\sinh \xi_0 + \sinh \xi_0 \cosh \xi_0 \ln \tanh \frac{\xi_0}{2} \right) \sin^2 \eta}{\frac{a}{c} + \frac{b^2}{c^2} \ln \frac{a+b-c}{a+b+c}} \quad (9)$$

Since for a Prolate spheroid $a = c \cosh \xi_0$, $b = c \sinh \xi_0$ (10)

But $\tanh \frac{\xi_0}{2} = \frac{a+b-c}{a+b+c} = \frac{b}{a+c}$ (11)

From (9) , (10) , and (11) , we get

$$\left(\frac{\partial \psi}{\partial \xi}\right)_{\xi=\xi_0} = U \sin^2 \eta \left[-ab + \frac{\frac{b^3}{c} + \frac{ab^3}{c^2} \ln \frac{b}{a+c}}{\frac{a}{c} + \frac{b^2}{c^2} \ln \frac{b}{a+c}} \right]$$

$$= U \sin^2 \eta \left[\frac{-cb}{\frac{a}{c} + \frac{b^2}{c^2} \ln \frac{b}{a+c}} \right] \quad (12)$$

and from (5) , (10) , and (11) , we obtain

$$\left(\frac{\partial \psi}{\partial \eta}\right)_{\xi=\xi_0} = 0 \quad (13)$$

Using (12) and (13) , (8) becomes

$$V^2 c^4 \sinh^2 \xi_0 \sin^2 \eta \left[\sinh^2 \xi_0 \cos^2 \eta + \cosh^2 \xi_0 \sin^2 \eta \right] = \frac{U^2 b^2 c^2 \sin^4 \eta}{\left[\frac{a}{c} + \frac{b^2}{c^2} \ln \frac{b}{a+c} \right]^2} \quad (14)$$

But from (1) and (2) , we get

$$\frac{z}{a} = \cos \eta , \quad \frac{r}{b} = \sin \eta \quad (15)$$

Using (10) , (15) in (14) , we have

$$V^2 = \frac{U^2 r^2 a^2 c^2}{\left[\frac{a}{c} + \frac{b^2}{c^2} \ln \frac{b}{a+c} \right]^2 (b^4 z^2 + a^4 r^2)} \quad (16)$$

Taking square root of (16) , the magnitude of exact velocity distribution over the boundary of a Prolate spheroid is given by

$$V = \frac{U a c r}{\left[\frac{a}{c} + \frac{b^2}{c^2} \ln \frac{b}{a+c} \right] \sqrt{b^4 z^2 + a^4 r^2}} \quad (17)$$

BOUNDARY CONDITIONS:

The boundary condition to be satisfied over the surface of a Prolate spheroid is

$$\frac{\partial \phi_{p.s}}{\partial n} = U \left(\hat{n} \cdot \hat{k} \right) \quad (18)$$

where $\phi_{p.s}$ is the perturbation velocity potential of a Prolate spheroid and $\hat{n}$ is the outward drawn unit normal to the surface of a Prolate spheroid

The equation of the boundary of the Prolate spheroid

$$\frac{z^2}{a^2}+\frac{y^2}{b^2}+\frac{x^2}{b^2} = 1$$

$$\text{Let} \quad f(x, y, z) = \frac{z^2}{a^2}+\frac{y^2}{b^2}+\frac{x^2}{b^2} - 1$$

$$\text{Then} \quad \nabla f = \frac{2x}{b^2}\hat{i}+\frac{2y}{b^2}\hat{j}+\frac{2z}{a^2}\hat{k}$$

$$\text{Therefore} \quad \hat{n} = \frac{\nabla f}{|\nabla f|} = \frac{\frac{2x}{b^2}\hat{i}+\frac{2y}{b^2}\hat{j}+\frac{2z}{a^2}\hat{k}}{\sqrt{\left(\frac{2z}{a^2}\right)^2+\left(\frac{2y}{b^2}\right)^2+\left(\frac{2x}{b^2}\right)^2}}$$

$$\text{Thus} \quad \hat{n}\cdot\hat{k} = \frac{\frac{2z}{a^2}}{\sqrt{\left(\frac{2z}{a^2}\right)^2+\left(\frac{2y}{b^2}\right)^2+\left(\frac{2x}{b^2}\right)^2}}$$

$$= \frac{\frac{z}{a^2}}{\sqrt{\frac{z^2}{a^4}+\frac{y^2}{b^4}+\frac{x^2}{b^4}}}$$

Therefore, the boundary condition in (18) takes the form

$$\frac{\partial \phi_{p.s}}{\partial n} = U\frac{\frac{z}{a^2}}{\frac{\sqrt{b^4 z^2 + a^4 y^2 + a^4 x^2}}{b^2 a^2}}$$

$$= \frac{z b^2}{\sqrt{b^4 z^2 + a^4 (y^2 + x^2)}} \quad \text{(Taking U = 1)} \qquad (19)$$

Equation (19) is the boundary condition, which must be satisfied over the boundary of a Prolate spheroid

For exterior flow for three-dimensional problems , the mathematical formulation for indirect boundary element method in terms of doublets distribution over the boundary ς of the body is given by

$$-\frac{1}{2}\Phi_i + \phi_\infty + \iint_{\varsigma - i} \Phi \frac{\partial}{\partial n}\left(\frac{1}{4\pi r}\right) d\varsigma = z_i \qquad (20)$$

Which is discretized by dividing the boundary of the body under consideration into 'm' elements and finally, it is written in matrix form as $[H] \{ \underline{U} \} = \{ \underline{R} \}$ (21)

Whereas usual [H] is a matrix of influence coefficients, $\{\underline{U}\}$ is a vector of unknown total potentials Φ_p and $\{ \underline{R} \}$ on the R.H.S. is a known vector whose elements are the negative of the values of the velocity potential of the uniform stream at the nodes on the boundary of the body.

METHOD OF ELEMENT DISTRIBUTION:

The indirect boundary element method is applied to calculate the potential flow solution around the prolate spheroid for which the analytical solution is available

Consider the surface of the sphere in one octant to be divided into three quadrilateral elements by joining the centroid of the surface with the mid points of the curves in the coordinate planes as shown in figure (2) (Mushtaq,M.et al,2009).

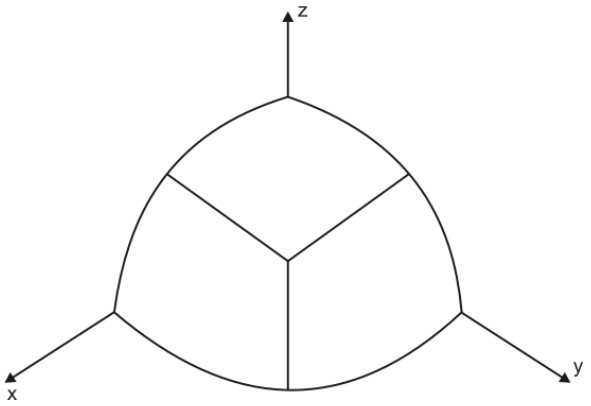

Figure (2)

Then each element is divided further into four elements by joining the centroid of that element with the mid–point of each side of the element. Thus one octant of the surface of the sphere is divided into 12 elements and the whole surface of the body is divided into 96 boundary elements. The above mentioned method is adopted in order to produce a uniform distribution of element over the surface of the body.

Figure (3) shows the method for finding the coordinate (x_p, y_p, z_p) of any point P on the surface of the sphere.

From figures (3) we have the following equation

$$\left|\vec{r}_p\right| = 1$$

$$\vec{r}_p \cdot \vec{r}_1 = \vec{r}_p \cdot \vec{r}_2$$

$$(\vec{r}_1 \times \vec{r}_2) \cdot \vec{r}_p = 0$$

or in cartesian form

$$x_p^2 + y_p^2 + z_p^2 = 1$$

$$x_p (x_1 - x_2) + y_p (y_1 - y_2) + z_p (z_1 - z_2) = 0$$

$$x_p (y_1 z_2 - z_1 y_2) + y_p (x_2 z_1 - x_1 z_2) + z_p (x_1 y_2 - x_2 y_1) = 0$$

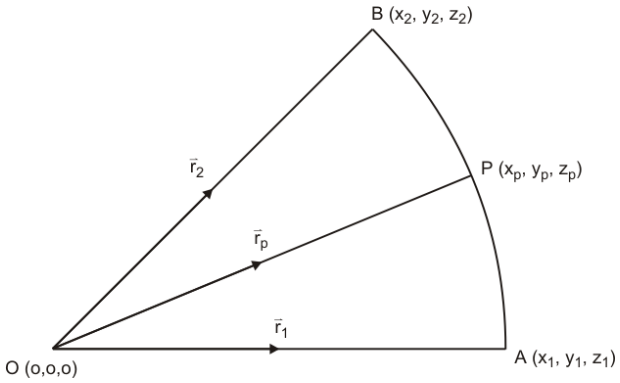

Figure (3)

As the body possesses planes of symmetry, this fact may be used in the input to the program and only the non–redundant portion need be specified by input points. The other portions are automatically taken into account. The planes of symmetry are taken to be the coordinate planes of the reference coordinate system. The advantage of the use of symmetry is that it reduces the order of the resulting system of equations and consequently reduces the

computing time in running a program. As a sphere is symmetric with respect to all three coordinate planes of the reference coordinate system, only one eighth of the body surface need be specified by the input points, while the other seven–eighth can be accounted for by symmetry.

The prolate spheroids of fineness ratios 2 and 10 are discretised into 24and 96 boundary elements and the computed velocity distributions are compared with analytical solutions for the prolate spheroids. In both cases of spheroids, the input points are distributed on the surface of a sphere and the x and y-coordinates of these points are then divided by the fineness ratios to generate the points for the prolate spheroids. The number of boundary elements used to obtain the computed velocity distribution is the same as are used for the sphere.

The calculated velocity distributions are compared with analytical solutions for the prolate spheroid of fineness ratios 2 and 10 using Fortran programming.

The following table (1) shows the comparison of the computed velocities with exact velocity over the surface of a prolate spheroid with fineness ratio 2 using 24 boundary elements.

TABLE 1

ELEMENT	XM	YM	ZM	R = $\sqrt{(YM)^2 + (ZM)^2}$	COMPUTED VELOCITY	EXACT VELOCITY
1	-.321E+00	-.374E+00	.161E+00	.40718E+00	.11669E+01	.11871E+01
2	-.748E+00	-.161E+00	.161E+00	.22769E+00	.77235E+00	.93409E+00
3	-.748E+00	.161E+00	.161E+00	.22769E+00	.77235E+00	.93409E+00
4	-.321E+00	.374E+00	.161E+00	.40718E+00	.11669E+01	.11871E+01
5	.321E+00	.374E+00	.161E+00	.40718E+00	.11669E+01	.11871E+01
6	.748E+00	.161E+00	.161E+00	.22769E+00	.77235E+00	.93409E+00
7	.748E+00	-.161E+00	.161E+00	.22769E+00	.77235E+00	.93409E+00
8	.321E+00	-.374E+00	.161E+00	.40718E+00	.11669E+01	.11871E+01
9	-.321E+00	-.161E+00	.374E+00	.40718E+00	.11669E+01	.11871E+01
10	-.321E+00	.161E+00	.374E+00	.40718E+00	.11669E+01	.11871E+01
11	.321E+00	.161E+00	.374E+00	.40718E+00	.11669E+01	.11871E+01
12	.321E+00	-.161E+00	.374E+00	.40718E+00	.11669E+01	.11871E+01

Graph 1

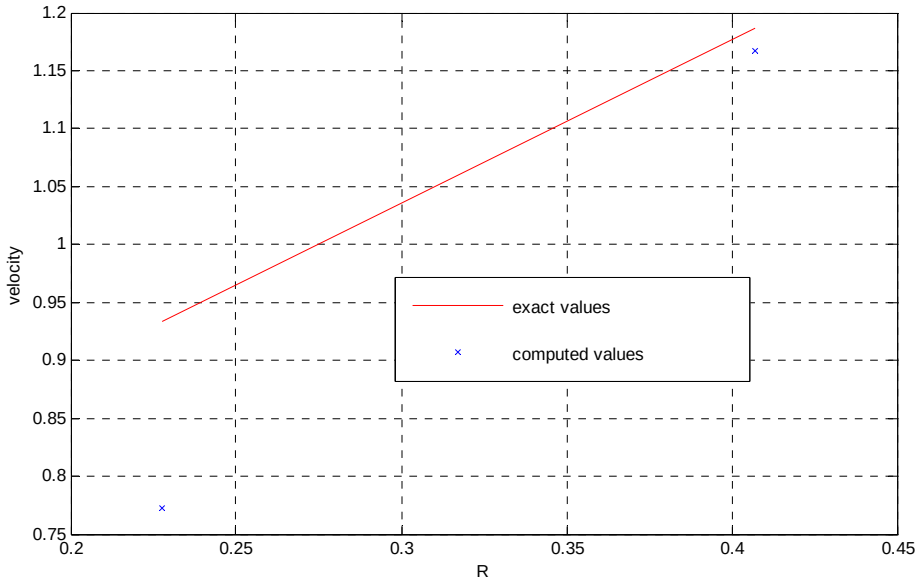

Comparison of computed and analytical velocity distributions over the surface of a prolate spheroid using 24 boundary elements with fineness ratio 2

The following table (2) shows the comparison of the computed velocities with exact velocity over the surface of a prolate spheroid with fineness ratio 10 using 24 elements.

TABLE 2

ELEMENT	XM	YM	ZM	R = $\sqrt{(YM)^2 + (ZM)^2}$	COMPUTED VELOCITY	EXACT VELOCITY
1	-.321E+00	-.748E-01	.321E-01	.08139E+00	.10315E+01	.10199E+01
2	-.748E+00	-.321E-01	.321E-01	.04539E+00	.94676E+00	.10071E+01
3	-.748E+00	.321E-01	.321E-01	.04539E+00	.94676E+00	.10071E+01
4	-.321E+00	.748E-01	.321E-01	.08139E+00	.10315E+01	.10199E+01
5	.321E+00	.748E-01	.321E-01	.08139E+00	.10315E+01	.10199E+01
6	.748E+00	.321E-01	.321E-01	.04539E+00	.94676E+00	.10071E+01
7	.748E+00	-.321E-01	.321E-01	.04539E+00	.94676E+00	.10071E+01
8	.321E+00	-.748E-01	.321E-01	.08139E+00	.10315E+01	.10199E+01
9	-.321E+00	-.321E-01	.748E-01	.08139E+00	.10315E+01	.10199E+01
10	-.321E+00	.321E-01	.748E-01	.08139E+00	.10315E+01	.10199E+01
11	.321E+00	.321E-01	.748E-01	.08139E+00	.10315E+01	.10199E+01
12	.321E+00	-.321E-01	.748E-01	.08139E+00	.10315E+01	.10199E+01

Graph 2

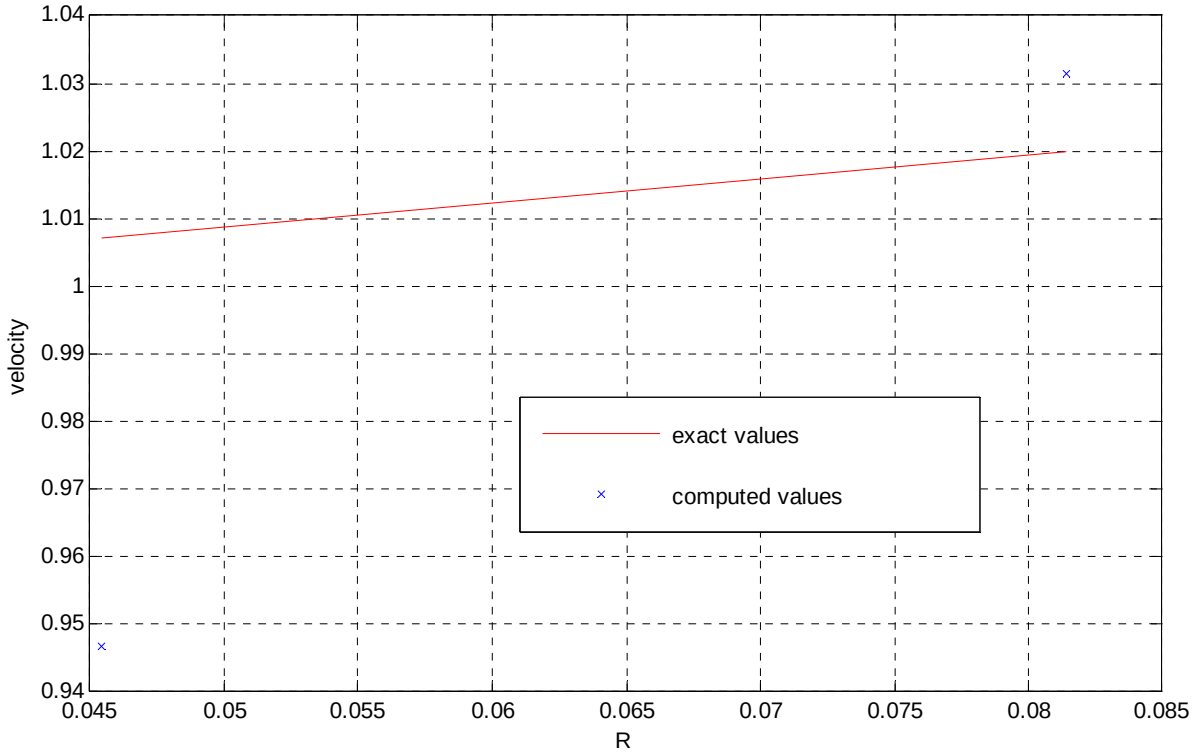

Comparison of computed and analytical velocity distributions over the surface of a prolate spheroid using 24 boundary elements with fineness ratio 10

The following table (3) shows the comparison of the computed velocities with exact velocity over the surface of a prolate spheroid with fineness ratio 2 using 96 boundary elements.

TABLE 3

ELEMENT	XM	YM	ZM	R = $\sqrt{(YM)^2 + (ZM)^2}$	COMPUTED VELOCITY	EXACT VELOCITY
1	-.177E+00	-.467E+00	.885E-01	.47529E+00	.12038E+01	.12048E+01
2	-.522E+00	-.399E+00	.785E-01	.40676E+00	.11455E+01	.11521E+01
3	-.798E+00	-.261E+00	.785E-01	.27264E+00	.94257E+00	.97640E+00
4	-.934E+00	-.885E-01	.885E-01	.12511E+00	.48460E+00	.57150E+00
5	-.934E+00	.885E-01	.885E-01	.12511E+00	.48460E+00	.57150E+00
6	-.798E+00	.261E+00	.785E-01	.27264E+00	.94257E+00	.97640E+00
7	-.522E+00	.399E+00	.785E-01	.40676E+00	.11455E+01	.11521E+01
8	-.177E+00	.467E+00	.885E-01	.47529E+00	.12038E+01	.12048E+01
9	.177E+00	.467E+00	.885E-01	.47529E+00	.12038E+01	.12048E+01
10	.522E+00	.399E+00	.785E-01	.40676E+00	.11455E+01	.11521E+01
11	.798E+00	.261E+00	.785E-01	.27264E+00	.94257E+00	.97640E+00
12	.934E+00	.885E-01	.885E-01	.12511E+00	.48460E+00	.57150E+00
13	.934E+00	-.885E-01	.885E-01	.12511E+00	.48460E+00	.57150E+00
14	.798E+00	-.261E+00	.785E-01	.27264E+00	.94257E+00	.97640E+00
15	.522E+00	-.399E+00	.785E-01	.40676E+00	.11455E+01	.11521E+01
16	.177E+00	-.467E+00	.885E-01	.47529E+00	.12038E+01	.12048E+01
17	-.157E+00	-.399E+00	.261E+00	.47693E+00	.12001E+01	.12059E+01
18	-.470E+00	-.352E+00	.235E+00	.42289E+00	.11630E+01	.11659E+01
19	-.703E+00	-.235E+00	.235E+00	.33220E+00	.10325E+01	.10695E+01
20	-.798E+00	-.785E-01	.261E+00	.27264E+00	.94257E+00	.97640E+00
21	-.798E+00	.785E-01	.261E+00	.27264E+00	.94257E+00	.97640E+00
22	-.703E+00	.235E+00	.235E+00	.33220E+00	.10325E+01	.10695E+01
23	-.470E+00	.352E+00	.235E+00	.42289E+00	.11630E+01	.11659E+01
24	-.157E+00	.399E+00	.261E+00	.47693E+00	.12001E+01	.12059E+01
25	.157E+00	.399E+00	.261E+00	.47693E+00	.12001E+01	.12059E+01
26	.470E+00	.352E+00	.235E+00	.42289E+00	.11630E+01	.11659E+01
27	.703E+00	.235E+00	.235E+00	.33220E+00	.10325E+01	.10695E+01
28	.798E+00	.785E-01	.261E+00	.27264E+00	.94257E+00	.97640E+00
29	.798E+00	-.785E-01	.261E+00	.27264E+00	.94257E+00	.97640E+00
30	.703E+00	-.235E+00	.235E+00	.33220E+00	.10325E+01	.10695E+01
31	.470E+00	-.352E+00	.235E+00	.42289E+00	.11630E+01	.11659E+01
32	.157E+00	-.399E+00	.261E+00	.47693E+00	.12001E+01	.12059E+01
33	-.157E+00	-.261E+00	.399E+00	.47693E+00	.12001E+01	.12059E+01
34	-.470E+00	-.235E+00	.352E+00	.42289E+00	.11630E+01	.11659E+01
35	-.522E+00	-.785E-01	.399E+00	.40676E+00	.11455E+01	.11521E+01
36	-.522E+00	.785E-01	.399E+00	.40676E+00	.11455E+01	.11521E+01
37	-.470E+00	.235E+00	.352E+00	.42289E+00	.11630E+01	.11659E+01
38	-.157E+00	.261E+00	.399E+00	.47693E+00	.12001E+01	.12059E+01
39	.157E+00	.261E+00	.399E+00	.47693E+00	.12001E+01	.12059E+01
40	.470E+00	.235E+00	.352E+00	.42289E+00	.11630E+01	.11659E+01
41	.522E+00	.785E-01	.399E+00	.40676E+00	.11455E+01	.11521E+01
42	.522E+00	-.785E-01	.399E+00	.40676E+00	.11455E+01	.11521E+01
43	.470E+00	-.235E+00	.352E+00	.42289E+00	.11630E+01	.11659E+01
44	.157E+00	-.261E+00	.399E+00	.47693E+00	.12001E+01	.12059E+01
45	-.177E+00	-.885E-01	.467E+00	.47529E+00	.12038E+01	.12048E+01
46	-.177E+00	.885E-01	.467E+00	.47529E+00	.12038E+01	.12048E+01
47	.177E+00	.885E-01	.467E+00	.47529E+00	.12038E+01	.12048E+01

48	.177E+00	-.885E-01	.467E+00	.47529E+00	.12038E+01	.12048E+01

Graph 3

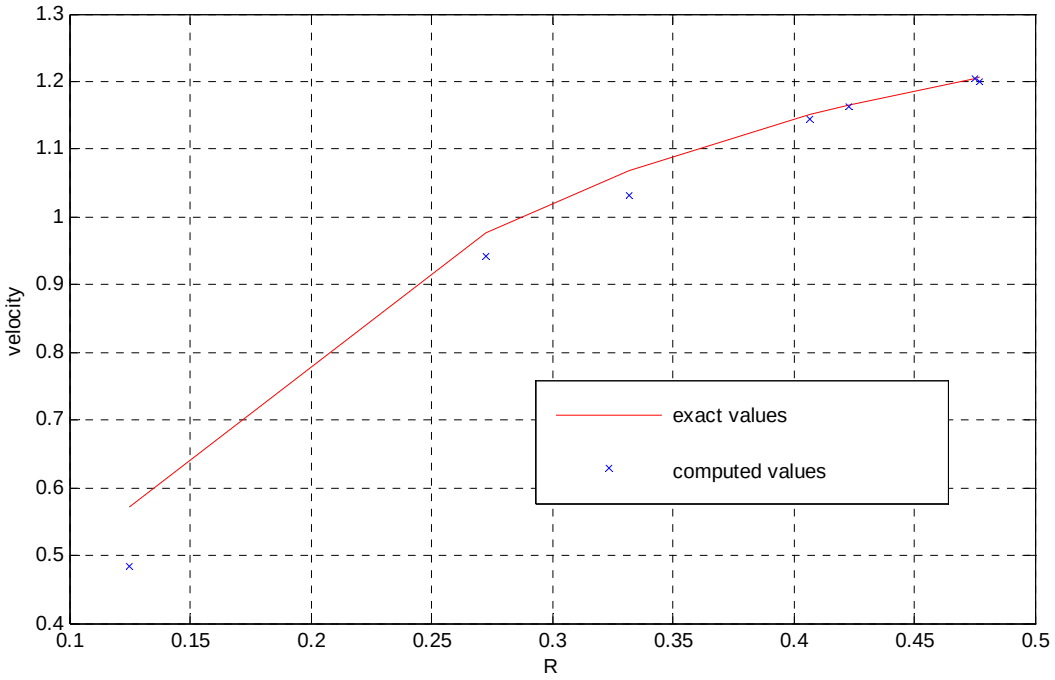

Comparison of computed and analytical velocity distributions over the surface of a prolate spheroid using 96 boundary elements with fineness ratio 2

The following table (4) shows the comparison of the computed velocities with exact velocity over the surface of a prolate spheroid with fineness ratio 10 using 96 boundary elements.

TABLE 4

ELEMENT	XM	YM	ZM	R = $\sqrt{(YM)^2 + (ZM)^2}$	COMPUTED VELOCITY	EXACT VELOCITY
1	-.177E+00	-.934E-01	.177E-01	.95057E-01	.10261E+01	.10205E+01
2	-.522E+00	-.798E-01	.157E-01	.81353E-01	.10256E+01	.10186E+01
3	-.798E+00	-.522E-01	.157E-01	.54527E-01	.10027E+01	.10099E+01
4	-.934E+00	-.177E-01	.177E-01	.25022E-01	.86585E+00	.95627E+00
5	-.934E+00	.177E-01	.177E-01	.25022E-01	.86585E+00	.95627E+00
6	-.798E+00	.522E-01	.157E-01	.54527E-01	.10027E+01	.10099E+01
7	-.522E+00	.798E-01	.157E-01	.81353E-01	.10256E+01	.10186E+01
8	-.177E+00	.934E-01	.177E-01	.95057E-01	.10261E+01	.10205E+01
9	.177E+00	.934E-01	.177E-01	.95057E-01	.10261E+01	.10205E+01
10	.522E+00	.798E-01	.157E-01	.81353E-01	.10256E+01	.10186E+01
11	.798E+00	.522E-01	.157E-01	.54527E-01	.10027E+01	.10099E+01
12	.934E+00	.177E-01	.177E-01	.25022E-01	.86585E+00	.95627E+00
13	.934E+00	-.177E-01	.177E-01	.25022E-01	.86585E+00	.95627E+00
14	.798E+00	-.522E-01	.157E-01	.54527E-01	.10027E+01	.10099E+01
15	.522E+00	-.798E-01	.157E-01	.81353E-01	.10256E+01	.10186E+01
16	.177E+00	-.934E-01	.177E-01	.95057E-01	.10261E+01	.10205E+01

17	-.157E+00	-.798E-01	.522E-01	.95386E-01	.10202E+01	.10206E+01
18	-.470E+00	-.703E-01	.470E-01	.84578E-01	.10247E+01	.10191E+01
19	-.703E+00	-.470E-01	.470E-01	.66440E-01	.10478E+01	.10150E+01
20	-.798E+00	-.157E-01	.522E-01	.54527E-01	.10027E+01	.10099E+01
21	-.798E+00	.157E-01	.522E-01	.54527E-01	.10027E+01	.10099E+01
22	-.703E+00	.470E-01	.470E-01	.66440E-01	.10478E+01	.10150E+01
23	-.470E+00	.703E-01	.470E-01	.84578E-01	.10247E+01	.10191E+01
24	-.157E+00	.798E-01	.522E-01	.95386E-01	.10202E+01	.10206E+01
25	.157E+00	.798E-01	.522E-01	.95386E-01	.10202E+01	.10206E+01
26	.470E+00	.703E-01	.470E-01	.84578E-01	.10247E+01	.10191E+01
27	.703E+00	.470E-01	.470E-01	.66440E-01	.10478E+01	.10150E+01
28	.798E+00	.157E-01	.522E-01	.54527E-01	.10027E+01	.10099E+01
29	.798E+00	-.157E-01	.522E-01	.54527E-01	.10027E+01	.10099E+01
30	.703E+00	-.470E-01	.470E-01	.66440E-01	.10478E+01	.10150E+01
31	.470E+00	-.703E-01	.470E-01	.84578E-01	.10247E+01	.10191E+01
32	.157E+00	-.798E-01	.522E-01	.95386E-01	.10202E+01	.10206E+01
33	-.157E+00	-.522E-01	.798E-01	.95386E-01	.10202E+01	.10206E+01
34	-.470E+00	-.470E-01	.703E-01	.84578E-01	.10247E+01	.10191E+01
35	-.522E+00	-.157E-01	.798E-01	.81353E-01	.10256E+01	.10186E+01
36	-.522E+00	.157E-01	.798E-01	.81353E-01	.10256E+01	.10186E+01
37	-.470E+00	.470E-01	.703E-01	.84578E-01	.10247E+01	.10191E+01
38	-.157E+00	.522E-01	.798E-01	.95386E-01	.10202E+01	.10206E+01
39	.157E+00	.522E-01	.798E-01	.95386E-01	.10202E+01	.10206E+01
40	.470E+00	.470E-01	.703E-01	.84578E-01	.10247E+01	.10191E+01
41	.522E+00	.157E-01	.798E-01	.81353E-01	.10256E+01	.10186E+01
42	.522E+00	-.157E-01	.798E-01	.81353E-01	.10256E+01	.10186E+01
43	.470E+00	-.470E-01	.703E-01	.84578E-01	.10247E+01	.10191E+01
44	.157E+00	-.522E-01	.798E-01	.95386E-01	.10202E+01	.10206E+01
45	-.177E+00	-.177E-01	.934E-01	.95057E-01	.10261E+01	.10205E+01
46	-.177E+00	.177E-01	.934E-01	.95057E-01	.10261E+01	.10205E+01
47	.177E+00	.177E-01	.934E-01	.95057E-01	.10261E+01	.10205E+01
48	.177E+00	-.177E-01	.934E-01	.95057E-01	.10261E+01	.10205E+01

Graph 4

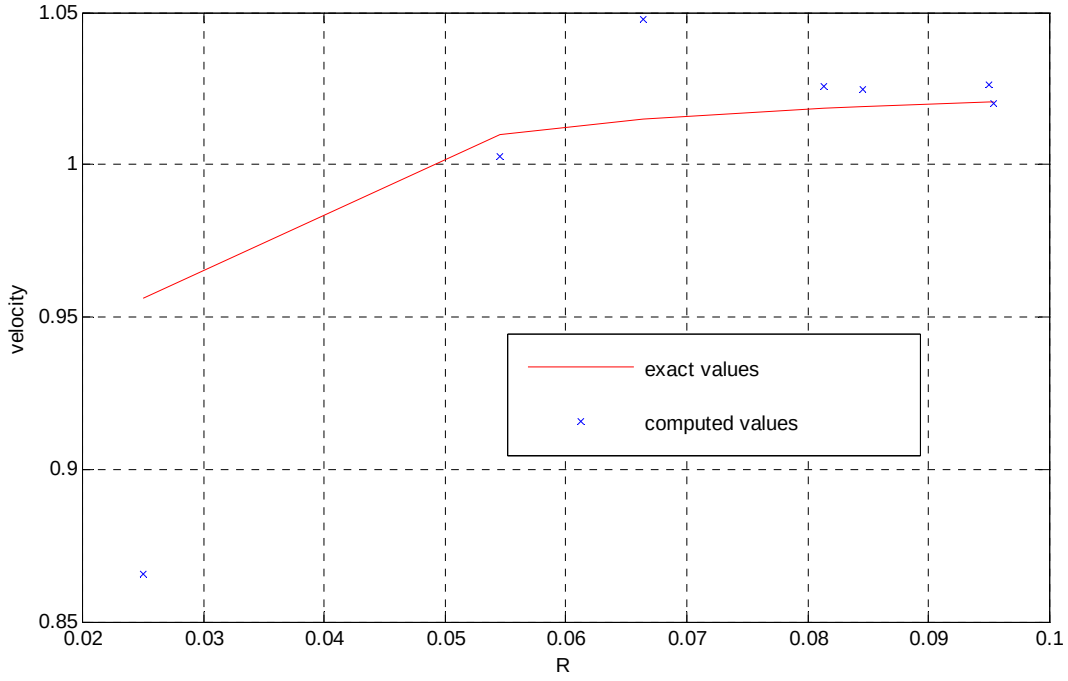

Comparison of computed and analytical velocity distributions over the Surface of a Prolate spheroid using 96 boundary elements with fineness ratio 10

Graphs 1 and 3 show the comparison of the computed and analytical distributions over the surface of a prolate spheroid of fineness ratio 2 for 24 and 96 boundary elements respectively. The graphs 2 and 4 show the comparison of the computed and analytical distributions over the surface of a prolate spheroid of fineness ratio 10 for 24 and 96 boundary elements respectively. The accuracy has increased with the increase of number of boundary elements and fineness ratio.

CONCLUSION:

An indirect boundary element method (IDBEM) is applied for calculation of an incompressible potential flow around a prolate spheroid. The computed results for flow velocities obtained by this method are compared with the analytical solutions for flow past a prolate spheroid. It is found from tables and graphs that the computed results for velocity distribution in both cases of prolate spheroids of fineness ratios 2 and 10 are seen to be quite good in agreement with the analytical results and the accuracy of results increases with the rise of number of boundary elements and fineness ratio. Indirect direct can be very useful in modeling bodies of complicated types like airplanes, road vehicles, space shuttle, missiles ,ships and submarines, etc.

REFERENCES:

Brebbia, C.A.: “The Boundary element Method for Engineers”, Pentech Press 1978.

Hirt, C.W. and Ramshaw, W.H.: “ Prospects for numerical simulation of bluff body aerodynamics”, Proceeding of the G.M.-Sympoium. Aerodynamic Drag Mechanisms of Bluff-Bodies and Road Vehicles, Plenum Press 1978.

Markatos, N.G. : "The theoretical prediction of the external aerodynamics of road vehicles", Int. J of vehicle design, technological advances in vehicle design series, SP3, impact of aerodynamics on vehicle design 1983, 378-400.

Demuran,A.O and Rodi, W.: " Calculations of three-dimensional turbulent flow around car bodies".‘Proceedings of the international symposium on 'Vehicle aerodynamics', Volkswagenwerk AG,1982.

Ecer, A. : 'The application of finite element methods for the prediction of flow around road vehicle", Proceedings of the international symposium on 'Vehicle aerodynamics', Volkswagenwerk AG,1982.

Lamb, H.: “Hydrodynamics” 6^{th} , Edition, Cambridge University Press 1932.

Milne-Thomson, L.M.: “Theoretical Hydrodynamics”, 5^{th} Edition, London Macmillan & Co. Ltd.,1968, 56-57.

Kellogg, O.D.: “Foundations of Potential Theory”, Frederick Ungar Publishing Company ,1929.

Brebbia, C.A. and Walker, S.: “ Boundary Element Techniques in Engineering” , Newnes-Butterworths, 1980.

Hess, J.L. and Smith, A.M.O.: “Calculation of non-lifting potential flow about three-dimensional bodies”, McDonnel Douglas Report No.E.S.40622,1962.

Hess, J.L. and Smith, A.M.O.: “Calculation of potential flow about arbitrary bodies”, Progress in Aeronautical Sciences, 8,1967, 1-158.

Morino L., Chen, Lee-Tzong and Suciu,E.O.: “A steady and oscillatory subsonic and supersonic aerodynamics around complex configuration”, AIAA Journal, 13,1975, 368-374.

Muhammad, G.; Shah, N.A. and. Mushtaq, M. . Advances and challenges to boundary element methods for incompressible viscous fluid flow problems, Aust. J. of Basic and Applied Sc. (in press),2009.

Shah, N.A. :Ideal Fuild Dynamics,A-One Publishers,Lahore-Pakistan,2008,545-553.

Mushtaq,M. , Shah, N.A & Muhammad, G : Comparison of Direct and Indirect Boundary Element Methods for the Flow Past a Sphere, Krag J. of Sc., 2009.